Density oscillation in highly flattened quantum elliptic rings and tunable strong dipole radiation

S.P. Situ, Y.Z. He, and C.G. Bao*
The State Key Laboratory of Optoelectronic Materials and Technologies, Zhongshan University, Guangzhou, 510275, P.R. China

A narrow elliptic ring containing an electron threaded by a magnetic field B is studied. When the ring is highly flattened, the increase of B would lead to a big energy gap between the ground and excited states, and therefore lead to a strong emission of dipole photons. The photon frequency can be tuned in a wide range by changing B and/or the shape of the ellipse. The particle density is found to oscillate from a pattern of distribution to another pattern back and forth against B. This is a new kind of Aharonov-Bohm oscillation originating from symmetry breaking and is different from the usual oscillation of persistent current.

*Corresponding author

It is recognized that micro-devices are important to micro-techniques. Various kinds of micro-devices, including the quantum rings,[1] have been extensively studied theoretically and experimentally in recent years. Quantum rings are different from other devices due to their special geometry. A distinguished phenomenon of the ring is the Aharonov-Bohm (A-B) oscillation of the ground state energy and persistent current[2−5]. It is believed that geometry would affect the properties of small systems. Therefore, in addition to circular rings, elliptic rings or other rings subjected to specific topological transformations deserve to be studied, because new and special properties might be found. There have been a number of literatures devoted to elliptic quantum dots[6−9] and rings[10−12]. It was found that the elliptic rings have two distinguished features. (i) The avoided crossing of the levels and the suppression of the A-B oscillation. (ii) The appearance of localized states which are related to bound states in infinite wires with bends.[13] These feature would become more explicit if the eccentricity is larger and the ring is narrower.

On the other hand, as a micro-device, the optical property is obviously essential to its application. It is guessed that very narrow rings with a high eccentricity might have special optical property, this is a point to be clarified. This paper is dedicated to this topic. It turns out that the optical properties of a highly flattened narrow ring is greatly different from a circular ring due to having a tunable energy gap, which would lead to strong dipole transitions with wave length tunable in a very broad range (say, from 0.1 to 0.001cm). Besides, a kind of A-B density-oscillation originating from symmetry breaking was found as reported as follows.

We consider an electron with an effective mass m^* confined on a one-dimensional elliptic ring with a half major axis r_{ax} and an eccentricity ε. Let us introduce an argument θ so that a point (x, y) at the ring is related to θ as $x = r_{ax}\cos\theta$ and $y = r_{ay}\sin\theta$, where $r_{ay} = r_{ax}\sqrt{1-\varepsilon^2}$ is the half minor axis. A uniform magnetic field B confined inside a cylinder with radius r_{in} vertical to the plane of the ring is applied. The associated vector potential reads $\mathbf{A} = Br_{in}^2\mathbf{t}/2r$, where $\mathbf{t}$ is a unit vector normal to the position vector $\mathbf{r}$. Then, the Hamiltonian reads

$$H = G/(1-\varepsilon^2\cos^2\theta)[-\frac{d^2}{d\theta^2} - i2\alpha\frac{\sqrt{1-\varepsilon^2}}{(1-\varepsilon^2\sin^2\theta)}\frac{d}{d\theta} + \alpha^2\frac{1-\varepsilon^2\cos^2\theta}{1-\varepsilon^2\sin^2\theta}] \quad (1)$$

where $G = \hbar^2/(2m^*r_{ax}^2)$, $\alpha = \phi/\phi_o$, $\phi = \pi r_{in}^2 B$ is the flux, $\phi_o = hc/e$ is the flux quantum.

The eigen-states are expanded as $\Psi_j = \sum_{k=k_{\min}}^{k_{\max}} C_k^{(j)} e^{ik\theta}$, where k is an integer ranging from $k_{\min}$ to $k_{\max}$, and $j = 1, 2, \cdots$ denotes the ground state, the second state, and so on. The coefficients $C_k^{(j)}$ are obtained via the diagonalization of H. In practice, B takes positive values, $k_{\min} = -100$ and $k_{\max} = 10$. This range of k assures the numerical results having at least four effective figures. The energy of the $j-th$ state is

$$E_j = \langle H\rangle_j \equiv \int d\theta(1-\varepsilon^2\cos^2\theta)\Psi_j^* H\Psi_j \quad (2)$$

where the eigen-state is normalized as

$$1 = \int d\theta(1-\varepsilon^2\cos^2\theta)\Psi_j^*\Psi_j \quad (3)$$

In the follows the units meV, nm, and Tesla are used, $m^* = 0.063m_e$ (for InGaAs rings), and r_{in} is fixed at 25. When $r_{ax} = 50$, $\varepsilon = 0$ and 0.4, the evolution of the low-lying spectra with B are given in Fig.1. When $\varepsilon = 0.4$, the effect of eccentricity is still small, the spectrum is changed only slightly from the case $\varepsilon = 0$, but the avoided crossing of levels can be seen.[10,11] In particular, the A-B oscillation exists and the period of ϕ remains to be ϕ_o. However, when ε becomes large, three remarkable changes emerge as shown in Fig.2. (i) The A-B oscillation of the ground state vanishes gradually. (ii) The energy of the second state becomes closer and closer to the ground state. (iii) There is an energy gap lying between the ground state and the third state, the

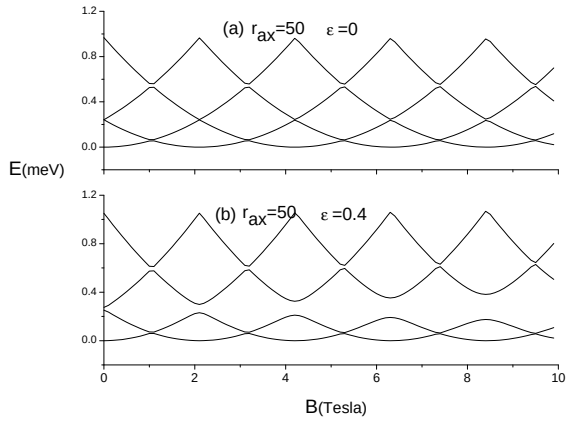

FIG. 1: Low-lying spectrum (in meV) of an one-electron system on an elliptic ring against B. $r_{ax} = 50nm$ and $\varepsilon = 0$ (a) and 0.4 (b). The period of the flux $\phi_o = hc/e$ is associated with $B = 2.106\ Tesla$.

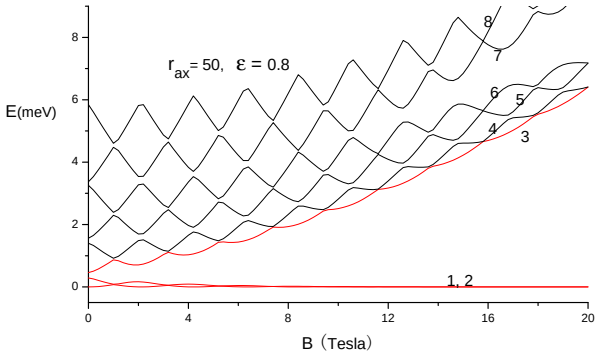

FIG. 2: Similar to Fig.1 but $\varepsilon = 0.8$. The lowest eight levels are included, where a great energy gap lies between the ground and the third states.

gap width increases nearly linearly with B. The existence of the gap is a remarkable feature which has not yet been found before from the rings with a finite width. This feature is crucial to the optical properties as shown later. Fig.3 demonstrates further how the gap varies with ε, r_{ax}, and B , where B is from 0 to 30 (or ϕ from 0 to $14.24\phi_o$). One can see that, when ε is large and r_{ax} is small, the increase of B would lead to a very large gap.

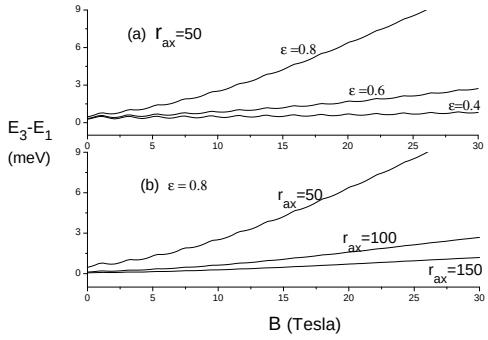

FIG. 3: Evolution of the energy gap $E_3 - E_1$ when r_{ax} and ε are given.

The A-B oscillation of the ground state energy is given in Fig.4. The change of ε does not affect the period (2.106 Tesla). However, when ε is large, the amplitude of the oscillation would be rapidly suppressed. Thus, for a highly flattened elliptic ring, the A-B oscillation appears only when B is small.

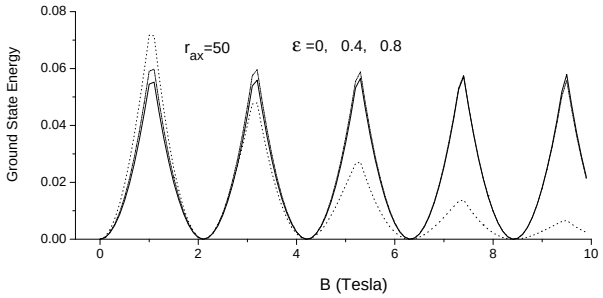

FIG. 4: The A-B oscillation of the ground state energy. The solid, dash-dot-dot, and dot lines are for $\varepsilon = 0$, 0.4, and 0.8, respectively.

The persistent current of the $j-th$ state reads[14]

$$J_j = G/\hbar[\Psi_j^*(-i\frac{d}{d\theta} + \alpha\frac{\sqrt{1-\varepsilon^2}}{(1-\varepsilon^2\sin^2\theta)})\Psi_j + c.c.] \quad (4)$$

The A-B oscillation of J_j is plotted in Fig.5. When ε is small (≤ 0.4), just as in Fig.4, the effect of ε is small as shown in 5a. When ε is large there are three noticeable points: (i) The oscillation of the ground state current would become weaker and weaker when B increases. (ii) The current of the second state has a similar amplitude as the ground state, but in opposite phase. (iii) The third (and higher) state has a much stronger oscillation of current.

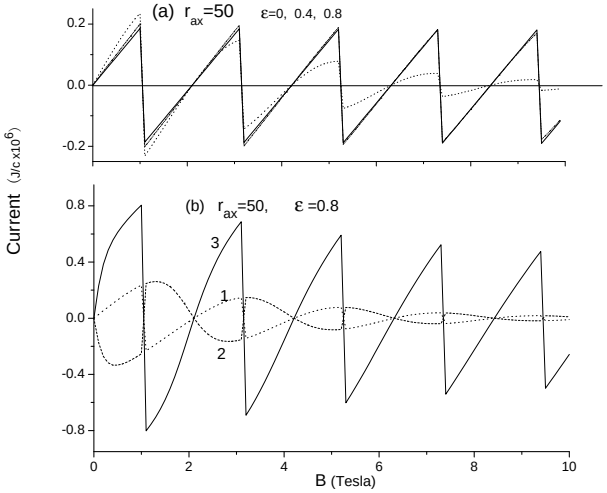

FIG. 5: The A-B oscillation of the persistent current J. (a) is for the ground state with $\varepsilon = 0$ (solid line), 0.4 (dash-dot-dot), and 0.8 (dot). (b) is for the first (ground), second and third states (marked by 1,2, and 3 by the curves) with ε fixed at 0.8. The ordinate is 10^6 times J/c in nm^{-1}.

For elliptic rings, the angular momentum L is not con-

served. However, it is useful to define $(\bar{L})_j = \langle -i\frac{\partial}{\partial\theta}\rangle_j$ (refer to eq.(2)). This quantity would tend to an integer if $\varepsilon \to 0$. It was found that (i) When ε is small (≤ 0.4), $(\bar{L})_1$ of the ground state decreases step by step with B, each step by one, just as the case of circular rings. However, when ε is large, $(\bar{L})_1$ decreases continuously and nearly linearly. (ii) When ε is small, $|(\bar{L})_i - (\bar{L})_1|$ is close (not close) to 1 if $2 \leq i \leq 3$ (otherwise). Since L would be changed by ± 1 under a dipole transition, the ground state would therefore essentially jump to the second and third states. Accordingly, the dipole photon has essentially two energies, namely, $E_2 - E_1$ and $E_3 - E_1$. However, this is not exactly true when ε is large.

There is a relation between the dipole photon energies and the persistent current.[15] For $\varepsilon = 0$, the ground state with $L = k_1$ would have the current $J_1 = G(k_1 + \alpha)/\pi\hbar$, while the ground state energy $E(k_1) = G(k_1 + \alpha)^2$. Accordingly the second and third states would have $L = k_1 \pm 1$, therefore we have

$$|E_3 - E_2| = |E(k_1 + 1) - E(k_1 - 1)| = 2hJ_1 \qquad (5)$$

This relation implies that the current can be accurately measured simply by measuring the energy difference of the photons emitted in dipole transitions. For elliptic rings, this relation holds approximately when ε is small (≤ 0.4), as shown in Fig.6a. However, the deviation is quite large when ε is large as shown in 6c.

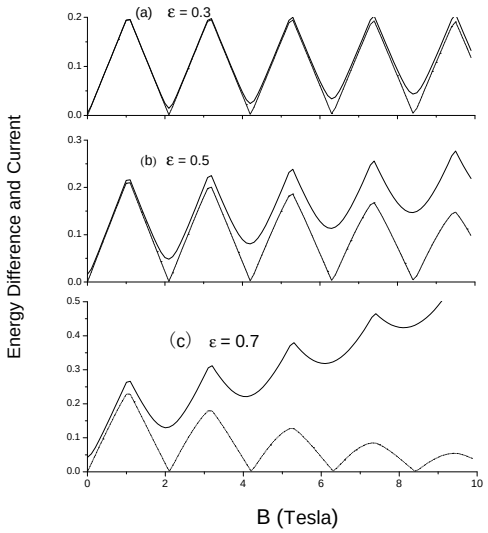

FIG. 6: $E_3 - E_2$ and the persistent current of the ground state. The solid line denotes $(E_3 - E_2)/(2hc)10^6$, the dash-dot-dot line denotes $|J|/c{\cdot}10^6$. They overlap nearly if $\varepsilon < 0.3$.

The probability of dipole transition from Ψ_j to $\Psi_{j'}$ reads

$$P^{\pm}_{j',j} = \frac{2e^2}{3\hbar}(\omega/c)^3 |\langle x \mp iy\rangle_{j',j}|^2 \qquad (6)$$

where $\hbar\omega = E_{j'} - E_j$ is the photon energy,

$$\langle x \mp iy\rangle_{j',j} = r_{ax}\int d\theta(1 - \varepsilon^2\cos^2\theta)\Psi^*_{j'} [\cos\theta \mp i\sqrt{1-\varepsilon^2}\sin\theta]\Psi_j \qquad (7)$$

The probability of the transition of the ground state to the $j' - th$ state is shown in Fig.7. When ε is small (≤ 0.4) and B is not very large (≤ 10), the allowed final states essentially Ψ_2 and Ψ_3, and the oscillation of the probability is similar to the case of circular rings with the same period as shown in 7a and 7b. In particular, $P^{\pm}_{3,1}$ is considerably larger than $P^{\pm}_{2,1}$ due to having a larger photon energy, thus the third state is particularly important to the optical properties. When ε is large (Fig.7c), the oscillation disappears gradually with B,while the probability increases very rapidly due to the factor $(\omega/c)^3$. Since $E_3 - E_1$ is nearly proportional to B as shown in Fig.3, the probability is nearly proportional to B^3. This leads to a very strong emission (absorption). Furthermore, in Fig.7c the black solid curve is much higher than the dash-dot-dot curve, it implies that the final states can be higher than Ψ_3, this leads to an even larger probability.

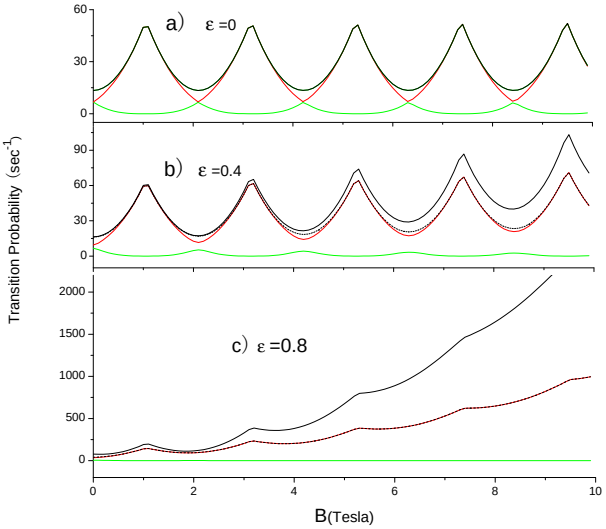

FIG. 7: Evolution of the probability of dipole transition of the ground state. The green line is for Ψ_1 to Ψ_2 transition, red line for Ψ_1 to Ψ_3, dash-dot-dot line is for the sum of the above two, solid line in black is for the total probability.

For circular rings, the particle densities ρ of all the eigen-states are uniform under arbitrary B. However, for elliptic rings, ρ is no more uniform as shown in Fig.8. For the ground state (8a), when ϕ =0, the non-uniformity is slight and ρ is a little smaller at the two ends of the major axis ($\theta = 0, \pi$). When ϕ increases, the density at the two ends of the minor axis ($\theta = \pi/2, 3\pi/2$) increases as well. When $\phi = 4\phi_o$ the non-uniformity is very strong as shown by the curve 9, where $\rho \approx 0$ when $\theta \approx 0$ or π. The second state has a parity opposite to the ground state,

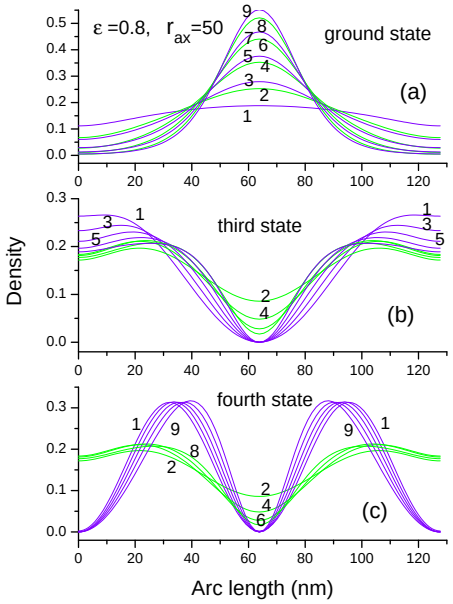

FIG. 8: Particle densities ρ as functions of the arc length (the according change of θ is 0 to π). The fluxes are given as $\phi = (i-1)\phi_o/2$, where i is an integer from 1 to 9 marked by the curves. The first group of curves (in violet) have $\phi/\phi_o =$ integer, the second group (in green) have $\phi/\phi_o =$ half-integer. When ϕ increases, the curve of ρ jumps from the first group to the second group and jumps back, and repeatedly.

but their densities are similar. For the third state (8b), ρ is peaked not at the ends of the major and minor axes but in between. In particular, when B increases, ρ oscillates from one pattern (say, in violet line) to another pattern (in green line), and repeatedly. The density oscillation would become stronger in higher states (8c). The period of oscillation remains to be ϕ_o, thus it is a new type of A-B oscillation without analogue in circular rings (where ρ remains uniform). Incidentally, the density oscillation does not need to be driven by a strong field, instead, a small change of ϕ from 0 to ϕ_o is sufficient.

Let us evaluate E_j roughly by using $(\bar{L})_j$ to replace the operator $-i\frac{\partial}{\partial\theta}$ in eq.(2) Then,

$$E_j \approx G\int d\theta\{[(\bar{L})_j + \alpha\frac{\sqrt{1-\varepsilon^2}}{1-\varepsilon^2\sin^2\theta}]^2 + [\frac{\alpha\varepsilon^2\sin 2\theta}{2(1-\varepsilon^2\sin^2\theta)}]^2\}\Psi_j^*\Psi_j \quad (8)$$

There are two terms at the right each is a square of a pair of brackets (for circular rings the second term does not exist). It is reminded that, while $\alpha = \phi/\phi_o$ is given positive, $(\bar{L})_j$ is negative. Thus there is a cancellation inside the first term. Therefore, when ε and α are large, the second term would be more important. It is recalled that both Ψ_1 and Ψ_2 are mainly distributed around $\theta = \pi/2$ and $3\pi/2$ (refer to Fig.8a), where the second term is zero due to the factor $\sin 2\theta$. Accordingly the energies of Ψ_1 and Ψ_2 are lower. On the contrary, both Ψ_3 and Ψ_4 are distributed close to the peaks of the second term (refer to Fig.8b and 8c), this leads to a higher energy. This effect would be greatly amplified by $\alpha\varepsilon^2$, this leads to the large energy gap shown in Fig.3.

In summary, the optical property of highly flattened elliptic narrow rings was found to be greatly different from circular rings. For the latter, both the energy of the dipole photon and the probability of transition are low, and they are oscillating in small domains. On the contrary, for the former, both the energy and the probability are not limited, the energy (probability) is nearly proportional to B (B^3), they are tunable by changing ε, r_{ax} and/or B. It implies that a strong source of light with frequency adjustable in a wide domain can be designed by using highly flattened, narrow, and small rings. Furthermore, a new type of A-B oscillation, namely, the density oscillation, originating from symmetry breaking, was found. This is a noticeable point because the density oscillation might be popular for the systems with broken symmetry (e.g., with C_3 symmetry).

Acknowledgment: The support under the grants 10574163 and 90306016 by NSFC is appreciated.

References

1, S.Viefers, P. Koskinen, P. Singha Deo, M. Manninen, Physica E **21** , 1 (2004)

2, U.F. Keyser, C. Fühner, S. Borck, R.J. Haug, M. Bichler, G. Abstreiter, and W. Wegscheider, Phys. Rev. Lett. **90**, 196601 (2003)

3, D. Mailly, C. Chapelier, and A. Benoit, Phys. Rev. Lett. **70**, 2020 (1993)

4, A. Fuhrer, S. Lüscher, T. Ihn, T. Heinzel, K. Ensslin, W. Wegscheider, and M. Bichler, Nature (London) **413**, 822 (2001)

5, A.E. Hansen, A. Kristensen, S. Pedersen, C.B. Sorensen, and P.E. Lindelof, Physica E (Amsterdam) **12**, 770 (2002)

6, M. van den Broek, F.M. Peeters, Physica E,**11**, 345 (2001)

7, E. Lipparini, L. Serra, A. Puente, European Phys. J. B **27**, 409 (2002)

8, J. Even, S. Loualiche, P. Miska, J. of Phys.: Cond. Matt., **15**, 8737 (2003)

9, C. Yannouleas, U. Landman, Physica Status Solidi A **203**, 1160 (2006)

10, D. Berman, O Entin-Wohlman, and M. Ya. Azbel, Phys. Rev. B **42**, 9299 (1990)

11, D. Gridin, A.T.I. Adamou, and R.V. Craster, Phys. Rev. B **69**, 155317 (2004)

12, A. Bruno-Alfonso, and A. Latgé, Phys. Rev. B **71**, 125312 (2005)

13, J. Goldstone and R.L. Jaffe, Phys. Rev. B **45**, 14100 (1992)

14, Eq.(4) originates from a 2-dimensional system via the following steps. (i) the components of the current

along X- and Y-axis are firstly obtained from the conservation of mass as well known. (ii) Then, the component along the tangent of ellipse j_θ can be obtained. (iii) j_θ is integrated along the normal of the ellipse under the assumption that the wave function is restricted in a very narrow region along the normal, then it leads to eq.(4).

15, Y.Z. He, C.G. Bao (submitted to PRB)